Abstract. In this paper, we study the requirements on orbit determination compatible with operation of next generation space clocks at their expected uncertainty. Using the ACES (Atomic Clock Ensemble in Space) mission as an example, we develop a relativistic model for time and frequency transfer to investigate the effects of orbit determination errors. We show that, for the considered orbit error models, the required uncertainty goal can be reached with relatively modest constraints on the orbit determination of the space clock, significantly less stringent than expected from "naive" estimates. Our results are generic to all space clocks and represent a significant step towards the generalized use of next generation space clocks in fundamental physics, geodesy, and time/frequency metrology.

Key words: Relativity - Reference systems - Time - Ephemerides

A&A manuscript no.
(will be inserted by hand later)

Your thesaurus codes are:
missing; you have not inserted them

ASTRONOMY AND ASTROPHYSICS

May 3, 2009

Orbit determination for next generation space clocks

Loïc Duchayne[1], **Flavien Mercier**[2], **and Peter Wolf**[1]

[1] LNE-SYRTE, Observatoire de Paris, CNRS, UPMC
[2] Centre National d'Etudes Spatiales

May 3, 2009

1. Introduction

Over the last decade of the 20^{th} century and the first few years of the 21^{st}, the uncertainty of atomic clocks has decreased by over two orders of magnitude, passing from the low 10^{-14} to below 10^{-16}, in relative frequency (Bize S. et al. 2005; Heavner T.P. et al. 2005; Oskay W.H. et al. 2006; Rosenband T. et al. 2008). This rapid evolution is essentially due to recent technological breakthroughs (laser cooling and trapping of atoms and ions), which allow very effective control and reduction of the motion of the atoms and correspondingly long interrogation times. Atomic fountain microwave clocks use freely falling laser cooled atoms and were the first to reach uncertainties below 10^{-15} some of them being at present in the low 10^{-16} range. They are now closely followed, and even surpassed, by trapped ion and neutral atom optical clocks, the best of which show uncertainties below 10^{-16}.

Space applications in fundamental physics, geodesy, time and frequency metrology, navigation, etc... are among the most promising for this new generation of clocks. Onboard terrestrial or solar system satellites, their exceptional frequency stability and accuracy make them a prime tool to test the fundamental laws of nature, and to study the Earth's and solar system gravitational potential and its evolution. In the longer term, they are likely to provide the primary time reference for the Earth, as clocks on the ground will be subject to the less accurate knowledge of the geopotential on the surface (Wolf P. and Petit G. 1995).

For example, when comparing a clock on a low Earth orbiting satellite ($\approx$ 1000 km altitude) to one on the ground they display a difference of $\approx 10^{-10}$ in relative frequency due to the relativistic gravitational frequency shift. Measuring that difference with 10^{-17} uncertainty would allow a test of the gravitational frequency shift to a few parts in 10^7 or equivalently, a determination of the potential difference between the clocks at the 10 cm level. The latter would contribute significantly to the knowledge of the geopotential and related applications in geophysics, representing the first realisation of relativistic geodesy (Bjerhammar A. 1985; Soffel M. et al. 1998) where the fundamental observable is directly the gravitational potential via the relativistic redshift.

From the above it is obvious that next generation space clocks at the envisaged uncertainty level require a fully relativistic analysis and modelling, not only of the clocks (in space and on the ground) but also of the time/frequency transfer method used to compare them (Allan D.W. and Ashby N. 1986; Klioner S.A. 1992; Petit G. and Wolf P. 1994; Wolf P. and Petit G. 1995; Blanchet L. et al. 2001; Linet B. and Teyssandier P. 2002). Indeed, a highly accurate space clock is of limited use unless it can be compared to ground clocks using a method that does not degrade the overall uncertainty, and unless the behaviour of the clocks as a function of their positions and velocities can be modelled with sufficient accuracy. As an example, simple order of magnitude estimates of the relativistic gravitational frequency shift show that an 1 m error on the position of the clocks leads to an error of $\approx 10^{-16}$ in the determination of their frequency difference. Similarly when using an one-way system (GPS like) for the time transfer an 1 m position error leads to an error of $\approx 3 \times 10^{-9}$ s in the synchronisation ie. $\geq 10^{-14}$ in relative frequency over one day.

In this paper, we study in more detail the requirements on orbit determination compatible with operation of next generation space clocks at the required uncertainty, and based on a completely relativistic model. We use the example of the ACES (Atomic Clock Ensemble in Space) mission, an ESA-CNES project to be installed onboard the ISS (International Space Station) in 2013. It consists of two atomic clocks and a two-way time transfer system (microwave link, MWL) with an overall uncertainty goal of 1 part in 10^{16} after ten day integration (see section 3 for more details). We show that the required accuracy goal can be reached with relatively modest constraints on the orbit determination of the space clock of $\approx$ 10 m in position (for the considered orbit error models), which is about an order of magnitude less stringent than expected from "naïve" estimates ($\approx$ 1 m, see above). This is due to first order cancellation between the velocity and position part of the orbit determination error in the determination of the relativistic frequency shift of the space clock, and to the use of a two-way time transfer system (MWL) which leads to first order cancellation of the position errors in the clock comparison (see section 6). Our results are generic to all space clocks (not limited to the ACES mission) and represent a significant step towards the generalised

use of next generation space clocks in fundamental physics, geodesy, and time/frequency metrology, as they show that the constraints on the orbit determination of the space clock are significantly less stringent than previously thought.

In sections 2 and 3 we briefly describe the ACES mission and the relativistic model used for the clocks and the time transfer. We explicitly derive the effect of orbit errors on the clock comparison in section 4. Up to this point, our results are completely general (within the specified approximations) with no assumptions on the expected orbit determination errors. We then apply those results using two examples of expected orbit errors (section 5). Our main results are the calculation of the effect of such orbit errors on the determination of the relativistic frequency shift of the clocks and on the time transfer (MWL) for the ACES mission (section 6). We provide the overall requirements on orbit determination for the ACES mission, and show that the mission objectives can be achieved with relatively modest performance on orbit determination. We discuss those results and conclude in section 7.

2. The ACES mission

The ACES project led by CNES and ESA aims at setting up on the ISS several highly stable clocks in 2013. The ACES payload includes two clocks, a hydrogen maser (SHM developed by TEMEX) and a cold atom clock PHARAO (developed by CNES) respectively for short and long term performances, and a microwave link for communication and time/frequency comparison. The frequency stability of PHARAO onboard the ISS is expected to be better than 10^{-13} for one second, $3\cdot10^{-16}$ over one day and $1\cdot10^{-16}$ over ten days, with an accuracy goal of $1\cdot10^{-16}$ in relative frequency.

The ACES mission has as objectives :

- to operate a cold atom clock in microgravity with a 100 mHz linewidth,
- to compare the high performances of the two atomic clocks in space (PHARAO and SHM) and to obtain a stability of $3\cdot10^{-16}$ over one day,
- to perform time comparisons between the two space clocks and ground clocks,
- to carry out tests of fundamental physics such as a gravitational redshift measurement and a test of Lorentz invariance, and to search for a possible drift of the fine structure constant α.
- to perform precise measurements of the Total Electron Content (TEC) in the ionosphere, the tropospheric delay and the Newtonian potential.

The time transfer is performed using a micro-wave two-way system, called Micro-Wave Link (MWL). An additional frequency is added in order to measure and correct the ionospheric delay at the required level. It uses carriers of frequency 13.5, 14.7 et 2.25 GHz, modulated by pseudo random codes respectively at $10^8\ s^{-1}$, $10^8\ s^{-1}$ and $10^6\ s^{-1}$ chip rates. Moreover it has four channels that allow four ground stations to be compared with the ISS clock at the same time.

According to the mission specifications, the microwave link has to synchronize two atomic clocks with a time stability of $\leq$ 0.3 ps over 300 s, $\leq$ 7 ps over one day, and $\leq$ 23 ps over 10 days. The performance of this link is a key issue since it will perform high precision time comparisons without damaging the high performances of the clocks.

For our purposes we express the above requirements for the MWL in a simplified form by the temporal Allan deviation ($\sigma_x(\tau)$) expressed in seconds:

$$\sigma_x(\tau) = 5.2\cdot10^{-12}\mathrm{s}\cdot\tau^{-\frac{1}{2}} \quad (1)$$

with the integration time τ in seconds. Equation (1) is valid for a single satellite pass over a ground station (for integration times τ lower than 300 s). For longer integrations times

$$\sigma_x(\tau) = 2.4\cdot10^{-14}\mathrm{s}\cdot\tau^{\frac{1}{2}}. \quad (2)$$

The temporal Allan deviation can be related to frequency instability as expressed by the modified Allan deviation $Mod\sigma_y(\tau)$ by

$$Mod\sigma_y(\tau) = \frac{\sqrt{3}\,\sigma_x(\tau)}{\tau}. \quad (3)$$

We take (1) and (2) as our upper limits for the calculation of all perturbing effects in the following sections, together with the overall accuracy requirement (maximum allowed frequency bias) of $1\cdot10^{-16}$ in relative frequency.

3. Relativistic model for clocks and time transfer of ACES

In a general relativistic framework each clock produces its own local proper time, in our case τ^g and τ^s for the ground and space clocks respectively.

In order to model signal propagation between the ground and the space stations, we use a non-rotating geocentric space-time coordinate system. Thus $t = x_0/c$ is the geocentric coordinate time, $\overrightarrow{x} = (x_1, x_2, x_3)$ are the spatial coordinates, where c is the speed of light in vacuum ($c = 299792458$ m.s^{-1}). We denote $U(t, \overrightarrow{x})$ as the total Newtonian potential at the coordinate time t and the position $\overrightarrow{x}$ with the convention that $U \geq 0$ (Soffel M. et al. 2003). In these coordinates, the metric is given by an approximate solution of Einstein's equations valid for low velocity and potential ($\frac{U}{c^2} << 1$ and $\frac{v^2}{c^2} << 1$):

$$ds^2 = -(1-\frac{2U(t,\overrightarrow{x})}{c^2})c^2dt^2 + (1+\frac{2U(t,\overrightarrow{x})}{c^2})d\overrightarrow{x}^2, \quad (4)$$

where higher order terms can be neglected for our purposes (Wolf P. and Petit G. 1995).

In this system, each emission or reception event (at the antenna phase center) is identified by its coordinate time t_i (figure 1) and a coordinate time interval is defined by $T_{ij} = t_j - t_i$. We define $\overrightarrow{x}_g$, $\overrightarrow{v}_g$ and $\overrightarrow{a}_g$ respectively as the position, the velocity and the acceleration of the ground station, and $\overrightarrow{x}_s$, $\overrightarrow{v}_s$ and $\overrightarrow{a}_s$ respectively as the position, the velocity and the acceleration of the space station.

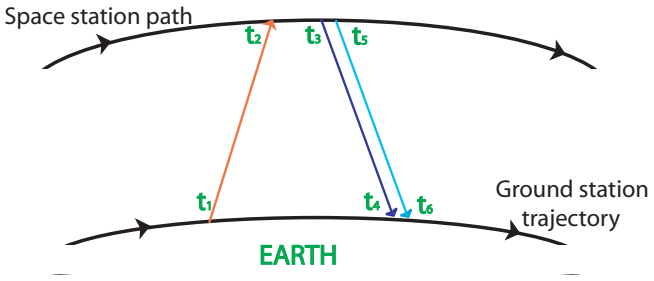

Fig. 1. MWL principle

The ACES mission uses two different antennas: one Ku-band antenna for uplink and downlink, and one S-band antenna for downwards signal only. The antennae are characterized by their phase pattern, which describes the position of the antenna phase center as a function of the direction of the incoming signal. The phase patterns of the MWL antennas have been measured in the laboratory at all three frequencies. For example, the phase variations with direction of the Ku-band antenna can reach up to $\sim$0.1 rad ($\sim$1 ps in time). Those variations can be corrected from the known phase pattern and a knowledge of ISS attitude (ie. direction of the incoming signal). Once corrected the remaining errors, mostly due to uncertainties in ISS attitude, are below the MWL specifications.

The f_1 frequency signal is emitted by the ground station at the coordinate time t_1 and received by the space station at t_2. The f_2 and f_3 frequency signals are emitted from the space station at t_3 and t_5, and received at the ground station at t_4 and t_6. The third frequency is added to measure the TEC in the ionosphere which allows the correction of the ionospheric delay.

The MWL is characterized by its continuous way of emission. It measures the time offsets between the locally generated signal and the received one. It provides three measurements (or observables) of the code (one on the space station, two on the ground) and three measurements of the phase of the carrier frequency at a sampling rate of one Hertz.

An observable is related to the phase comparison between a signal derived from the local oscillator and the received signal, corrected for the frequency difference mainly due to the first order Doppler effect (see Bahder T. B. 2003 for details of a similar procedure used in GPS). If we consider a particular bit of the signal which is produced locally at τ_p and received at τ_a, an observable is a measurement of the local proper time interval between these two events. The actual measurement of the phase difference $\Delta\Phi(\tau_a, \overrightarrow{x}_a)$ occurs at the single space-time point $(\tau_a, \overrightarrow{x}_a)$ and is labeled with the arrival proper time τ_a. It can be expressed as

$$\Delta\tau(\tau_a, \overrightarrow{x}_a) = \frac{\Delta\Phi(\tau_a, \overrightarrow{x}_a)}{\omega} + \delta\tau = \tau_p - \tau_a \qquad (5)$$

where ω is a conversion factor from phase to proper time depending on the nominal carrier and code frequencies, and $\delta\tau$ represents the measurement errors (difference between the clock and ideal proper time, measurement phase noise, etc...).

Considering the experimental uncertainties of the ACES mission (see equation (1) and (2)), we will neglect any terms in the relativistic model that, when maximised, lead to corrections of less than $3 \cdot 10^{-13}$ s in time. Numerical applications are necessary to evaluate which terms can be neglected. For this purpose, we consider the International Space Station with a circular trajectory at an altitude of 400 km in a plane inclined by 51.6^o with respect to the equatorial plane. It has a velocity $v_s = 7.7 \cdot 10^3\ m.s^{-1}$ in a gravitational potential of $U_s/c^2 = 6.5 \cdot 10^{-10}$. The ground station has a velocity $v_g = 465\ m.s^{-1}$ at a gravitational potential of $U_g/c^2 = 6.9 \cdot 10^{-10}$.

The tropospheric delay Δ^{tropo} is considered as independent of the frequency of the signal, with a slow variation with time and an amplitude of less than 100 ns.

We assume the density of electrons in the ionosphere N_e is less than $2 \cdot 10^{12}$ electrons/m^3. The ionospheric delay Δ^{iono} is maximum for the f_3 frequency signal with an amplitude of less than 10 ns.

The relation between the proper time τ and the coordinate time t is given to sufficient accuracy by

$$\frac{d\tau}{dt} = 1 - \left(\frac{U(t, \overrightarrow{x})}{c^2} + \frac{v^2(t)}{2c^2}\right) + O(c^{-4}). \qquad (6)$$

Higher order terms of equation (6) have negligible effects at the projected uncertainty of $1 \cdot 10^{-16}$ in relative frequency of the ACES clocks (Wolf P. and Petit G. 1995). Note however, that some care has to be taken when evaluating the Newtonian potential $U(t, \overrightarrow{x})$ in (6) for the ground or space clock (Wolf P. and Petit G. 1995).

The ACES mission aims at obtaining the variation of the desynchronisation between ground and space clocks with time, that is to say, the function $\tau^g(t) - \tau^s(t)$. It is evaluated by combining the measurements performed on the ground and onboard the space station and a precise calculation of the signal propagation times. In order to be able to control T_{23} (see below), we combine two measurements $\Delta\tau^s(\tau^s(t_2))$ and $\Delta\tau^g(\tau^g(t_4))$ but with $\tau^s(t_2) \neq \tau^g(t_4)$. Then the expression of desynchronisation reads (see (Duchayne L. 2008) for a detailed derivation)

$$\begin{aligned}\tau^g(t_a) - \tau^s(t_a) = \frac{1}{2}\Bigg(&\Delta\tau^s(\tau^s(t_2)) - \Delta\tau^g(\tau^g(t_4)) \\ &+ T_{12} - T_{34} \\ &- \int_{t_1}^{t_2} \left(\frac{U(t, \overrightarrow{x_g})}{c^2} + \frac{v_g^2(t)}{2c^2}\right) dt \\ &+ \int_{t_3}^{t_4} \left(\frac{U(t, \overrightarrow{x_s})}{c^2} + \frac{v_s^2(t)}{2c^2}\right) dt\Bigg),\end{aligned} \qquad (7)$$

where $t_a = \frac{t_2+t_4}{2}$, and where $\Delta\tau^s(\tau^s(t_2))$ and $\Delta\tau^g(\tau^g(t_4))$ are the observables respectively from the ground and onboard the satellite at the coordinate times t_2 and t_4, and where we have neglected non-linearities of $\tau^g(t)$ and $\tau^s(t)$ over the interval $t_4 - t_2$ (few milliseconds). The integral terms result from proper

time to coordinate time transformations. They are small corrections of order 10^{-12} s to the desynchronisation $\tau^g(t_a) - \tau^s(t_a)$.

However, it is the derivative with respect to the coordinate time t of the relation (7) which has to be studied for applications such as the gravitational redshift test or geodesy. Actually it has to be compared with the next relation obtained from equation (6):

$$\frac{d\tau^g}{dt} - \frac{d\tau^s}{dt} = \frac{1}{c^2}\cdot\left(U(t,\overrightarrow{x_s}) - U(t,\overrightarrow{x_g}) + \frac{v_s^2(t)}{2} - \frac{v_g^2(t)}{2}\right) + O(c^{-4}). \tag{8}$$

We note that any constant term appearing in the desynchronisation expression (7) will have no effect on the final result (8) because of the derivation.

In (7) the difference $T_{12} - T_{34}$ needs to be calculated from the knowledge of satellite and ground positions and velocities (orbit determination). For example, T_{12} is the time interval elapsed between emission from the ground station and reception by the satellite of the f_1 frequency signal. It can be written as

$$T_{12} = \frac{R_{12}}{c} + \frac{2GM_E}{c^3}\ln\left(\frac{x_g(t_1) + x_s(t_2) + R_{12}}{x_g(t_1) + x_s(t_2) - R_{12}}\right) + \Delta_{12}^{tropo} + \Delta_{12}^{iono} + O(\frac{1}{c^4}), \tag{9}$$

where $R_{12} = ||\overrightarrow{R_{12}}|| = ||\overrightarrow{x_s}(t_2) - \overrightarrow{x_g}(t_1)||$, where the logarithmic term represents the Shapiro time delay (Shapiro I. I. 1964) (see e.g. Blanchet L. et al. 2001 for a detailed derivation) and where Δ_{12}^{tropo} and Δ_{12}^{iono} are respectively the tropospheric and ionospheric delays on the signal path.

Only one of the clocks (here we assume the ground clock) has a known relation with coordinate time t, so $\overrightarrow{x}_s(t_2)$ cannot be directly obtained from the orbit determination, only $\overrightarrow{x}_s(t_1)$ is known. Relation (9) is then modified to

$$T_{12} = \frac{D(t_1)}{c} + \frac{\overrightarrow{D}(t_1).\overrightarrow{v_s}(t_1)}{c^2} + \frac{D(t_1)}{2c^3}\left(||\overrightarrow{v_s}(t_1)||^2 + \overrightarrow{D}(t_1).\overrightarrow{a_s}(t_1) + (\frac{\overrightarrow{D}(t_1).\overrightarrow{v_s}(t_1)}{D(t_1)})^2\right) + \frac{2GM_E}{c^3}\ln\left(\frac{x_g(t_1) + x_s(t_1) + D(t_1)}{x_g(t_1) + x_s(t_1) - D(t_1)}\right) + \Delta_{12}^{iono} + \Delta_{12}^{tropo} + O(c^{-4}), \tag{10}$$

where $\overrightarrow{D}(t) = \overrightarrow{x_s}(t) - \overrightarrow{x_g}(t)$, $D(t) = ||\overrightarrow{D}(t)||$, and where the unknown position $\overrightarrow{x_s}(t_2)$ in (9) was expanded in a Taylor series around the corresponding known position $\overrightarrow{x_s}(t_1)$. The ionospheric and tropospheric terms are related to the signal paths. They need to be calculated for $\overrightarrow{R}(t)$, but only $\overrightarrow{D}(t)$ is known. The corresponding correction is related to the motion of the space station during the atmospheric delay of the signal (the atmospheric equivalent of the "Sagnac" type term (2^{nd} term in (10)). The corresponding corrections to the tropospheric term and to the ionospheric terms at frequencies f_1 and f_2 are negligible but included for the f_3 signal (see equation (14)).

Assuming that $T_{23} \leq 10^{-3}$ s , the expression of $T_{12} - T_{34}$ where all terms greater than $3\cdot 10^{-13}$ s have been included when maximized for ACES can be evaluated by :

$$\begin{aligned} T_{12} - T_{34} = {} & 2\frac{\overrightarrow{D}(t_4).\overrightarrow{v_g}(t_4)}{c^2} + \frac{\overrightarrow{D}(t_4).\overrightarrow{\Delta v}(t_4)}{c\cdot D(t_4)}T_{23} \\ & + 2\frac{D(t_4)}{c^3}\cdot\left(\overrightarrow{\Delta v}(t_4).\overrightarrow{v_s}(t_4) - \overrightarrow{D}(t_4).\overrightarrow{a_g}(t_4) + \|\overrightarrow{\Delta v}(t_4)\|^2\right) \\ & + \frac{T_{23}}{c^2}\cdot\left(\overrightarrow{\Delta v}(t_4).\overrightarrow{v_s}(t_4) - \overrightarrow{D}(t_4).\overrightarrow{a_s}(t_4) + 2\|\overrightarrow{\Delta v}(t_4)\|^2 - 2\overrightarrow{D}(t_4).\overrightarrow{\Delta a}(t_4) - (\frac{\overrightarrow{D}(t_4).\overrightarrow{\Delta v}(t_4)}{D(t_4)})^2\right) \\ & + \frac{T_{23}^2}{2cD(t_4)}\left(\|\overrightarrow{\Delta v}(t_4)\|^2 - \overrightarrow{D}(t_4).\overrightarrow{\Delta a}(t_4) - (\frac{\overrightarrow{D}(t_4).\overrightarrow{\Delta v}(t_4)}{D(t_4)})^2\right) \\ & + \Delta_{12}^{iono} - \Delta_{34}^{iono} + O(\frac{1}{c^4}), \end{aligned} \tag{11}$$

where $\overrightarrow{\Delta v}(t) = \overrightarrow{v}_g(t) - \overrightarrow{v}_s(t)$ and $\overrightarrow{\Delta a}(t) = \overrightarrow{a}_g(t) - \overrightarrow{a}_s(t)$.

To obtain (11) we have applied (10) for the upward and downward signals and expanded all positions and velocities in Taylor series around their values at t_4, which can be obtained from the time of measurement ("label" of the observable $\Delta\tau^g(\tau^g(t_4))$ in (7)), on the ground.

The difference $T_{12} - T_{34}$ of upward and downward signals at f_1 and f_2 allows to eliminate to first order delaying and restraining factors such as range (D/c), troposphere or Shapiro effects. Due to the asymmetry of the paths, that cancellation is not perfect, and there are some terms left (equation (11)) which depend on orbit determination as well as on the coordinate time interval T_{23} elapsed between reception and emission at the phase centre of the MWL antenna onboard the ISS.

The time interval T_{23} can be controlled by "shifting" the time of the measurements on the ground or on board the space station (e.g. shifting $\tau^s(t_2)$ in $\Delta\tau^s(\tau^s(t_2))$ of equation (7)) when post-processing the data. That allows the control of the difference between emission and reception *at the clock*. But T_{23} in (11) is defined at the antenna phase centre, therefore its control requires the knowledge (calibration and in situ measurement) of the instrumental delays (cables, electronics, etc...) in

the MWL space segment. So the control and knowledge (uncertainty δT_{23}) of T_{23} is determined by the uncertainty of the calibration and measurement of internal delays, which will play a role in the following.

The ionospheric effect Δ^{iono} on a radio signal of frequency f can be modelled as follows (Bassiri S. and Hajj G. A. 1993):

$$\begin{aligned}\Delta^{iono} = & \frac{40.3082}{c \cdot f^2} \int N_e dL \\ & - \frac{7527}{f^3} \int (\overrightarrow{B}_0 . \overrightarrow{k}) \cdot N_e dL + O(\frac{1}{c^4}),\end{aligned} \tag{12}$$

where $\overrightarrow{B}_0$ is the Earth's magnetic field ($||\overrightarrow{B}_0|| \approx 3.12 \cdot 10^{-5} T$) and $\overrightarrow{k}$ is the direction of propagation of the signal.

The electron density integrated along the signal trajectory, $\int N_e dL$, is usually referred as the Total Electron Content (TEC). The difference of ionospheric delays appearing in equation (11) is then

$$\begin{aligned}\Delta^{iono}_{12} - \Delta^{iono}_{34} = & (\frac{1}{f_1^2} - \frac{1}{f_2^2}) \frac{40.3082}{c} TEC \\ & - \frac{7527}{f_1^3} \int \frac{\overrightarrow{B}_0 . \overrightarrow{D}(t_2)}{D(t_2)} N_e dL \\ & - \frac{7527}{f_2^3} \int \frac{\overrightarrow{B}_0 . \overrightarrow{D}(t_4)}{D(t_4)} N_e dL + O(\frac{1}{c^4}).\end{aligned} \tag{13}$$

The second and third term in (13) represent the effect of the Earth's magnetic field and amount to at most 0.5 ps for ACES, which is almost negligible. Therefore, an only very rough estimation of these terms is sufficient.

The TEC is determined by combining the two downwards signal observables. The time interval T_{46} elapsed between the receptions of the two signals depends on the differences of their internal delays at the emission from the space station (i.e. T_{35}) and on the difference of their propagation time. Assuming that $T_{46} < 1\ \mu s$, the expression of the Total Electron Content is then given by the following expression :

$$\begin{aligned}TEC = & \frac{c}{40.3082} \frac{1}{\frac{f_2^2 - f_3^2}{f_2^2 f_3^2} + \frac{f_2^3 - f_3^3}{f_2^3 f_3^3} \frac{7527 \cdot c}{40.3} \frac{\overrightarrow{B}_0 . \overrightarrow{D}(t_4)}{D(t_4)}} \times \\ & \left(\Delta\tau^g(\tau^g(t_4)) - \Delta\tau^g(\tau^g(t_6)) \right. \\ & \left. + \frac{\overrightarrow{D}(t_4) . \Delta\overrightarrow{v}(t_4)}{D(t_4)} \frac{T_{46}}{c} \right) / \left(1 - \right. \\ & \left. \frac{\overrightarrow{D}(t_4) . \overrightarrow{v_s}(t_4)}{D(t_4) \cdot c} \right) + O(\frac{1}{c^4}).\end{aligned} \tag{14}$$

The last term in (14) is negligible when used for the time transfer (when inserted into (13)) but may be significant for the study of the TEC itself.

In summary, a reliable orbit determination is required for two main reasons. On one hand to calculate precisely the corrections in equations (11). On the other hand, to evaluate correctly the terms on the right hand side of equation (8) ie. the second order Doppler and gravitational redshifts.

In addition, we also need a precise knowledge of the time interval T_{23}, (ie. of the onboard internal delays) in order to be able to calculate the corresponding terms in (11) with sufficient accuracy.

The aim of this work is to estimate using simple orbit error models, which levels of uncertainty on orbit determination and calibration of internal delays (knowledge of T_{23}) are required to reach the required performances. For that purpose only the leading terms in (11) are required ie.

$$\begin{aligned}T_{12} - T_{34} = & 2 \frac{\overrightarrow{D}(t_4) . \overrightarrow{v_g}(t_4)}{c^2} \\ & + \frac{\overrightarrow{D}(t_4) . \overrightarrow{\Delta v}(t_4)}{c \cdot D(t_4)} T_{23} + O(\frac{1}{c^3}),\end{aligned} \tag{15}$$

which, together with equation (8) for the relativistic frequency shift, is sufficient to derive the maximum allowed uncertainties on orbit determination and internal delays in order to stay below the limits given by (1) and (2).

4. Effects of orbit errors on clock comparison

We now use equations (15) and (8) to express the effects of station trajectory and time calibration uncertainties on the time transfer and on the relativistic frequency shift. In this section we make no assumptions on orbit determination errors, our results being completely general and valid up to the neglected terms as described below.

We note ($\overrightarrow{X}_a(t)$, $\overrightarrow{V}_a(t)$) and ($\overrightarrow{X}'_a(t)$, $\overrightarrow{V}'_a(t)$) respectively the true and computed trajectories of the antenna phase center, and ($\overrightarrow{X}_c(t)$, $\overrightarrow{V}_c(t)$) and ($\overrightarrow{X}'_c(t)$, $\overrightarrow{V}'_c(t)$) respectively the true and computed trajectories of the clock reference point. We also define ($\overrightarrow{X}_o(t)$, $\overrightarrow{V}_o(t)$) the true trajectory and the true velocity of the center of mass of the ISS. These five trajectories are expressed in the non-rotating geocentric frame (GCRS, Geocentric Celestial Reference System) (Soffel M. et al. 2003).

On one hand, the error in the time transfer is related with the uncertainties of $T_{12} - T_{34}$, and can be obtained from the simplified equation (15). It is then dependent on the ground and space station trajectory knowledge, on the value of T_{23} and on the uncertainty on this parameter δT_{23}. As said before, a precise knowledge of the time interval T_{23} is related to the internal delay calibrations. The error on $T_{12} - T_{34}$ is

$$\begin{aligned}\delta(T_{12} - T_{34}) = & 2 \frac{\delta\overrightarrow{D} . \overrightarrow{v_g} + \overrightarrow{D} . \delta\overrightarrow{v_g}}{c^2} + \frac{\overrightarrow{D} . \Delta\overrightarrow{v}}{c \cdot D} \delta T_{23} \\ & + \left(\frac{\delta\overrightarrow{D} . \Delta\overrightarrow{v}}{c \cdot D} + \frac{\overrightarrow{D} . \delta\Delta\overrightarrow{v}}{c \cdot D} \right. \\ & \left. - \frac{\overrightarrow{D} . \Delta\overrightarrow{v}}{c \cdot D} \frac{\delta D}{D} \right) T_{23}.\end{aligned} \tag{16}$$

In general ground station uncertainties are below 10 cm. Thus the uncertainty on ground station position is negligible with respect to the ISS position errors and the knowledge of the vector $\overrightarrow{D}$ is only related to the uncertainty of the space station reference point which is the antenna phase center. Then we have $\delta\overrightarrow{D} = \overrightarrow{X_a X'_a}$.

The previous equation can then be written as :

$$\begin{aligned}\delta\left(T_{12}-T_{34}\right) = 2\frac{\overrightarrow{X_a X'_a}.\overrightarrow{v_g}}{c^2} + \frac{\overrightarrow{D}.\overrightarrow{\Delta v}}{c\cdot D}\delta T_{23} \\ + \left(\frac{\overrightarrow{X_a X'_a}.\overrightarrow{\Delta v}}{c\cdot D} - \frac{\overrightarrow{D}}{c\cdot D}.\frac{d\overrightarrow{X_a X'_a}}{dt}\right. \\ \left. - \frac{\overrightarrow{D}.\overrightarrow{\Delta v}}{c\cdot D}\frac{\|\overrightarrow{X_a X'_a}\|}{D}\right) T_{23}.\end{aligned} \tag{17}$$

We note that equation (17) depends the antenna phase center position error ($\overrightarrow{X_a X'_a}$), the coordinate time interval T_{23} and the uncertainty on this time interval δT_{23}.

On the other hand, the clock relativistic correction along a trajectory is obtained from equation (8). It depends on the position and the velocity of the reference point, in this case the clock. We need to express the error on the reference point frequency - ie. the frequency difference between the true clock position and the computed clock position - in order to compare its Modified Allan deviation with the specifications.

The gravitational potential can be evaluated on a given trajectory with sufficient precision (Wolf P. and Petit G. 1995) using gravity models (eg. GRIM5 or EGM96). The error on the frequency shift at the clock position is given by :

$$\begin{aligned}\delta(\frac{d\tau}{dt})_{\overrightarrow{X_c}} &= (\frac{d\tau}{dt})_{\overrightarrow{X_c}} - (\frac{d\tau}{dt})_{\overrightarrow{X'_c}} \\ &= -\frac{1}{c^2}\left(U(t,\overrightarrow{X_c}) - U(t,\overrightarrow{X'_c})\right. \\ &\quad \left. + \frac{V_c^2 - V_c'^2}{2}\right).\end{aligned} \tag{18}$$

The frequency difference between the reference point position $\overrightarrow{X}$ and the ISS center of mass $\overrightarrow{X}_o$ is given by :

$$\begin{aligned}(\frac{d\tau}{dt})_{\overrightarrow{X}} - (\frac{d\tau}{dt})_{\overrightarrow{X}_o} = -\frac{1}{c^2}\left(U(t,\overrightarrow{X}) - U(t,\overrightarrow{X}_o)\right. \\ \left. + \frac{V^2 - V_o^2}{2}\right).\end{aligned} \tag{19}$$

The trajectory of $\overrightarrow{X}_o$ is the solution of the differential equation

$$\frac{d^2\overrightarrow{X}_o}{dt^2} = \overrightarrow{\Gamma}_P + \overrightarrow{\Gamma}_S, \tag{20}$$

where $\overrightarrow{\Gamma}_P$ is the acceleration due to the gravitational potential and $\overrightarrow{\Gamma}_S$ is the acceleration due to other effects (e.g. surface forces like air drag and radiation pressure).

Using

$$\overrightarrow{\Gamma}_P = \overrightarrow{Grad}(U), \tag{21}$$

and to first order

$$U(t,\overrightarrow{X}) = U(t,\overrightarrow{X}_o) + \overrightarrow{\Gamma}_P(\overrightarrow{X_o}).\overrightarrow{X_o X}, \tag{22}$$

and multiplying equation (20) by the vector $\overrightarrow{X_o X}$ (which is the position of the clock with respect to the ISS center of mass), we can substitute the difference of gravitational potential in equation (19) by :

$$\begin{aligned}U(t,\overrightarrow{X}) - U(t,\overrightarrow{X}_o) &= \overrightarrow{\Gamma}_P(\overrightarrow{X_o}).\overrightarrow{X_o X} \\ &= \frac{d^2\overrightarrow{X}_o}{dt^2}.\overrightarrow{X_o X} - \overrightarrow{\Gamma}_S.\overrightarrow{X_o X}.\end{aligned} \tag{23}$$

Then we obtain :

$$\begin{aligned}(\frac{d\tau}{dt})_{\overrightarrow{X}} - (\frac{d\tau}{dt})_{\overrightarrow{X}_o} = -\frac{1}{c^2}\left(\frac{d\overrightarrow{V}_o}{dt}.\overrightarrow{X_o X} + \overrightarrow{V_o}.\frac{d\overrightarrow{X_o X}}{dt}\right. \\ \left. + \frac{1}{2}(\frac{d\overrightarrow{X_o X}}{dt})^2 - \overrightarrow{\Gamma}_S.\overrightarrow{X_o X}\right),\end{aligned} \tag{24}$$

which can be simplified to :

$$\begin{aligned}(\frac{d\tau}{dt})_{\overrightarrow{X}} - (\frac{d\tau}{dt})_{\overrightarrow{X}_o} = -\frac{1}{c^2}\left(\frac{d}{dt}\left(\overrightarrow{V_o}.\overrightarrow{X_o X}\right)\right. \\ \left. + \frac{1}{2}(\frac{d\overrightarrow{X_o X}}{dt})^2 - \overrightarrow{\Gamma}_S.\overrightarrow{X_o X}\right).\end{aligned} \tag{25}$$

In this expression the term $\frac{1}{2}(\frac{d\overrightarrow{X_o X}}{dt})^2 - \overrightarrow{\Gamma}_S.\overrightarrow{X_o X}$ can be interpreted as the relativistic correction for the clock referenced to the local ISS frame. In fact, for an observer in the ISS frame, the non gravitational acceleration $\overrightarrow{\Gamma}_S$ produces an acceleration which can be seen by this observer as coming from a "gravitational potential" $-\overrightarrow{\Gamma}_S.\overrightarrow{X_o X}$. The term $\frac{d}{dt}\left(\overrightarrow{V_o}.\overrightarrow{X_o X}\right)$ is the position of the clock with respect to the ISS center of mass projected on the ISS velocity direction (along track component). If there are no external accelerations, and if the velocity of $\overrightarrow{X}$ in the ISS frame remains small, only this term is present.

Combining the previous equation with the same expressed in $\overrightarrow{X'}$, we obtain :

$$\begin{aligned}\delta(\frac{d\tau}{dt})_{\overrightarrow{X_c}} = \frac{1}{c^2}\left(\frac{d}{dt}\left(\overrightarrow{V_o}.\overrightarrow{X_c X'_c}\right) + \frac{1}{2}(\frac{d\overrightarrow{X_o X_c}}{dt})^2\right. \\ \left. - \frac{1}{2}(\frac{d\overrightarrow{X_o X'_c}}{dt})^2 - \overrightarrow{\Gamma}_S.\overrightarrow{X_c X'_c}\right).\end{aligned} \tag{26}$$

In order to simplify equation (26), we evaluate the order of magnitude of the different contributors appearing in this equation.

To investigate the importance of the non gravitational term $\frac{\overrightarrow{\Gamma}_S.\overrightarrow{X_c X'_c}}{c^2}$, the drag has been modeled along a reference orbit of

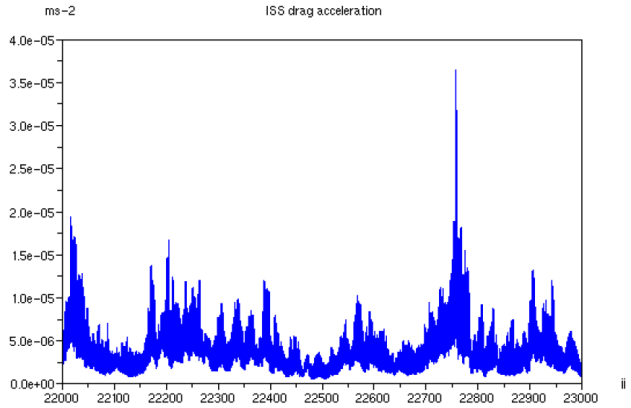

Fig. 2. Estimation of the non gravitational acceleration of the ISS vs time (in days)

the ISS. A period with important solar activity has been chosen in order to evaluate the worst case (see figure 2).

To estimate its effect on formula (26), the acceleration has been multiplied by a 10 meter bias, by a 10 meter random noise or by a 10 meter sinusoidal function at orbital period, corresponding to possible attitude and orbit error effects of the ISS. The Allan deviation stays below 10^{-21}, which is totally negligible here. Also, this term has no effect on the frequency accuracy at the 10^{-16} level aimed at by ACES. In addition, the residual term of the second order Doppler shift $\frac{1}{2c^2}\left[(\frac{d\overrightarrow{X_oX_c}}{dt})^2-(\frac{d\overrightarrow{X_oX_c'}}{dt})^2\right]$ must be computed with the GCRS trajectories. The order of magnitude of these terms can be evaluated as $\sim(a\delta a\Omega^2/c^2)$ with Ω the orbital angular frequency, $a=||\overrightarrow{X_oX_c}||$, and δa its error. For $a\leq 100$ m and $\delta a\leq 10$ m this effect is also totally negligible.

The only important term for the performance evaluation is thus the along track term $\frac{1}{c^2}\frac{d}{dt}\left(\overrightarrow{V_o}.\overrightarrow{X_cX_c'}\right)$, and equation (26) can be written :

$$\begin{aligned}\delta(\frac{d\tau}{dt})_{\overrightarrow{X_c}} &= (\frac{d\tau}{dt})_{\overrightarrow{X_c}}-(\frac{d\tau}{dt})_{\overrightarrow{X_c'}}\\ &= \frac{1}{c^2}\left[\frac{d}{dt}\left(\overrightarrow{V_o}.\overrightarrow{X_cX_c'}\right)\right].\end{aligned} \tag{27}$$

So only the component of the clock position error $\overrightarrow{X_cX_c'}$ projected on the velocity of the ISS $\overrightarrow{V_o}$ plays a role. This can be understood considering for example a purely positive radial component. In this case we underestimate the gravitational potential but overestimate the velocity, and the two cancel. We underline again the fact that the derivations in this chapter are valid for any type of orbital errors, up to the neglected terms described above.

The scalar products of vectors can be evaluated in a local frame : for example it may be useful to study them in the local orbital frame ($\overrightarrow{R}$, $\overrightarrow{T}$, $\overrightarrow{N}$) defined with $\overrightarrow{R}$ the unit vector between the Earth's center and the space station, $\overrightarrow{N}$ orthogonal to $\overrightarrow{R}$ and the inertial velocity, and $\overrightarrow{T}$ orthogonal to $\overrightarrow{R}$ and $\overrightarrow{N}$.

The ISS attitude is assumed to be roughly constant. The clock position error in this frame is represented by a constant vector (error in the position of the clock relative to the centre of mass), and by perturbations which reflect :

- attitude uncertainties (rigid body behaviour of ISS). If we take ± 5 degrees uncertainty and a distance of 10 meters, this leads to 0.87 meters amplitude error for the clock position.
- ISS deformations : they are due to thermoelastic effects which will be mainly at orbital period (eclipses and sun orientation). We suppose that these effects are below one meter amplitude.
- vibrations : here we suppose that the 'vibrations' are related to frequencies higher or equal to the first ISS eigenfrequency which is higher than the orbital period. The corresponding displacements remain small and are expected to stay below one meter.

Either of these effects is negligible when inserted into (17) and (27). So for our purposes the only significant contribution to the trajectory errors of the antenna phase center and the clock come from the position errors of the ISS center of mass.

In summary, the errors on the time transfer and on the relativistic correction have been expressed as functions of the trajectory knowledge through equations (17) and (27). Moreover, only the error in the knowledge of the ISS center of mass position has an importance in the relativistic correction.

5. Orbit error examples

In this section we describe two simple models for ISS orbit errors as examples to investigate numerically the effect they have on ACES performance.

We consider two methods used to evaluate the orbit of a satellite. On the one hand, the dynamical method takes into account the equations of motion to restitute the trajectory. It fits the measured data towards an orbit satisfying the principles of celestial mechanics and estimates a number of parameters which give the best fit trajectory. On the other hand, the kinematic method uses directly the measurements of the satellite position (eg. GPS data) with no a priori assumption of the form of the orbit. In both cases the resulting orbit errors are in general not easily described by a simple model, but for our purposes we use two examples that should approximately reflect the orders of magnitude of the main orbit error contributions.

For dynamical orbit determination the differences between true and computed trajectories of the ISS center of mass are expected to have specific structures. For example an eccentricity error gives no long term effects, but periodic errors can be important and the radial, along track and velocity errors are correlated. For weak eccentricity orbits, the difference between two real orbits is given by the Hill model (or the Clohessy-Wiltshire model) which is an expansion of uncertainties with respect to a reference circular orbit (Colombo O. L. 1986; Colombo O. L. et al. 2004). If we suppose there exists a set of parameters which perfectly describes the true orbit of the ISS,

then this model is a first approximation to the errors of the center of mass between the computed and the true orbits.

For kinematic orbit determination one expects little a priori correlation between the different orbit error components. We therefore use a simple independent random noise on each component as a first approximation.

In the Hill model the position uncertainties along radial, tangential and normal axis (in the local ISS frame) are given as follows:

$$\begin{aligned} \text{radial axis} &: \delta R(t) = \frac{1}{2} X \cdot \cos(\Omega t + \varphi_R) + c_R \\ \text{tangential axis} &: \delta T(t) = -X \cdot \sin(\Omega t + \varphi_R) - \frac{3}{2}\Omega \cdot c_R \cdot t + d_R \\ \text{normal axis} &: \delta N(t) = Y \cdot \cos(\Omega t + \varphi_N) \end{aligned} \tag{28}$$

where X, Y, c_R and d_R are amplitude coefficients, and where Ω is the orbital angular frequency. For our purpose, bias (d_R) plays no role and the linear term (c_R) depends on arc length. Basically the longer the observation duration is, the smaller this coefficient becomes. The main feature of this error model is to take into account the error correlations in the orbital plane. For instance, a positive radial bias leads to a negative error on the tangential velocity: the satellite is delayed with respect to the reference orbit.

6. Numerical results

We now use the previously described error models to calculate the corresponding constraints imposed by the ACES stability (equations (1) and (2)) and accuracy requirements, via equations (17) and (27). We first consider the Hill model, followed by results for a simple random noise.

We consider orbit error models in the local $(\vec{R}, \vec{T}, \vec{N})$ frame, so we need to transform them to GCRS and determine the uncertainties in this frame on position and on velocity parameters. We consider an ephemeris of the ISS corresponding to the 20^{th} of May, 2005 and a ground station based in Toulouse, France $(43^o36'N, 1^o26'E)$. Actually, this station has been chosen as the master ground station of the ACES mission. All station parameters and their uncertainties have to be expressed in the same frame (ie. GCRS).

We first consider the error equation (17) on the time transfer. We choose the signs of the independent parameters ($\overrightarrow{X_a X'_a}$, T_{23} and δT_{23}) so as to maximize the resulting temporal Allan deviation. The calculated deviation has to be compared with the MWL specifications.

Assuming we have no error on T_{23} (ie. $\delta T_{23} = 0$ s), for all values of factor X (or Y) of equation (28), it is possible to determine the maximum value of the time interval T_{23} for which the temporal Allan deviation remains under the specifications. With numerous values of X, we calculate a bound which marks out two different areas : the allowed uncertainties area in which each couple (X, T_{23}) gives a deviation staying under the specifications, and the prohibited area.

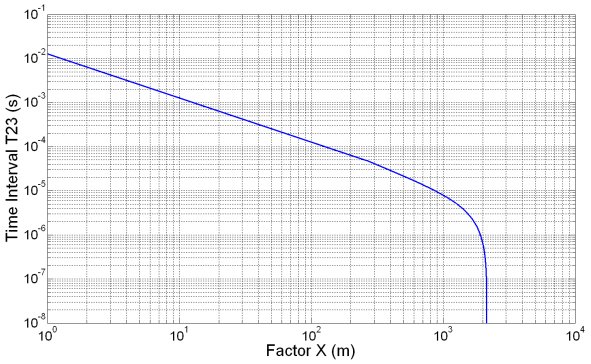

Fig. 3. Maximum allowed value of T_{23} as function of the scale factor X to comply with the specifications, assuming $\delta T_{23} = 0$

Figure 3 shows that, the smaller the time interval T_{23}, the larger the allowed uncertainty on the space station position. This result provides a way to combine upwards and downwards signals to allow the maximum uncertainty on space station position in order to comply with the specifications. The most favorable situation is when the reception at the antenna phase center of the space station corresponds to the emission at the same place ie. $t_2 = t_3$ (see figure 4). This way of combining signals is named the "Λ configuration". To work with parameters in the asymptotic area (see figure 3) requires T_{23} to be below 10^{-6} s.

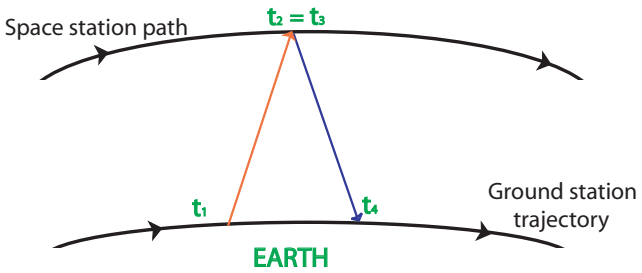

Fig. 4. The "Λ configuration" is the way to combine upwards and downwards signals which allows the maximum uncertainties on the space station orbit determination

Then if we plot the maximum value of δT_{23} for all values of the factor X, there will appear two asymptotic values we cannot cross if we want to stay within the specifications (see figure 5). Basically a compromise between the knowledge of the space station trajectory and the precision of the internal delays calibration must be achieved owing to the maximization of the Allan deviation. We will evaluate the maximum allowed errors on these two parameters if no other errors are present.

We search for the asymptotic value of factors X and Y which comply with the specifications for all phases (φ_R, φ_N) when we have no error on T_{23}. The asymptotic value for orbit

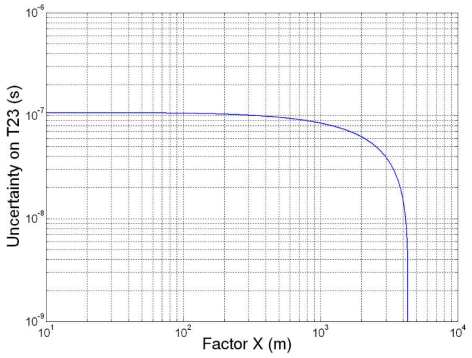

Fig. 5. Maximum allowed value of δT_{23} as function of the scale factor X to comply with the specifications, assuming $T_{23} = 0$

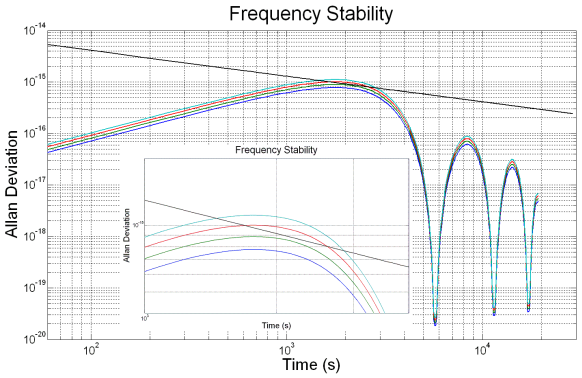

Fig. 7. Modified Allan deviations of the redshift error for X=14, 16, 18, 20 m

determination is obtained for $X, Y = 4200$ m which corresponds to a 4.2 km error on the tangential and normal axes, and to a 2.1 km error on the radial axis.

The asymptotic value of the time calibration does not depend on orbit determination uncertainties. So it is independent of the phases φ_R and φ_N. Then we can draw the temporal Allan deviations for different values of δT_{23} (see figure 6). We find that δT_{23} must stay below $1.06 \cdot 10^{-7}$ s.

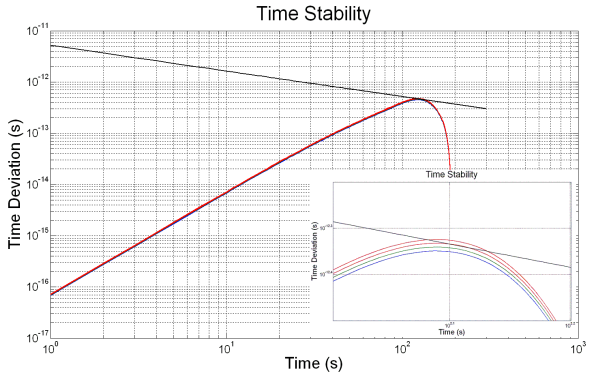

Fig. 6. Temporal Allan deviations for $X = 0$, $T_{23} = 0$ s and $\delta T_{23} = [102, 104, 106, 108]$ ns

The requirements for several passes have also been investigated. In this case, the calculated deviations have to be compared to the specifications given by (2). The results showed that the requirements on orbit determination and time calibration are less stringent for several passes than for a single pass. Therefore if specifications are respected for a single pass, specifications for longer integration times are also respected.

Now we evaluate requirements on orbit determination considering the relativistic frequency shift. We search for the maximum value of X to comply with the specifications (1) and (2). Equation (27) is evaluated with the error model (28), and its Allan deviation is calculated for different values of X. For integration times greater than one thousand seconds, these Allan deviations are independent of the phases φ_R and φ_N.

Figure 7 shows that, if the factor X in (28) is equal to 16 m ie. if we have an eight meter error on the radial axis and sixteen meter error on the tangential axis, then we comply with the specifications.

Because of the projection of the position error along the ISS center of mass velocity (see equation (27)), the requirement on the factor Y is orders of magnitude less stringent. The bound is given by the asymptotic value coming from the time transfer (see equation (17) and figure 5).

We now turn to the second example of orbit determination errors: independent random errors on $\overrightarrow{R}$, $\overrightarrow{T}$ and $\overrightarrow{N}$. We consider white noise of amplitude (standard deviation) δR, δT, δN at one second sampling intervals on each of the three components.

Similarly to the Hill model, the by far more stringent constraints come from the effect of these errors on the relativistic frequency shift via equation (27). In particular, a white noise δT in equation (27) will translate into a temporal Allan variance given by

$$\sigma_x(\tau) \simeq \frac{V_0 \delta T}{c^2} \cdot \tau^{-\frac{1}{2}}, \tag{29}$$

which satisfies the requirements (1) and (2) for all integration times when $\delta T \leq 60$ m.

Because of the projection of the error on $\overrightarrow{V_0}$ in (27) the relativistic frequency shift imposes virtually no limits on the normal and radial components of the errors. Those are limited by the effect on the time transfer given by equation (17). Assuming $T_{23} \leq 10^{-6}$ s and $\delta T_{23} \leq 10^{-7}$ s (see above) the first term of that equation is by far dominant. Maximizing the dot product in that term we obtain an upper limit of 1.4 km on δR and δN in order to stay within specifications for all integration times.

Finally, we consider the accuracy requirement of ACES i.e. 10^{-16} in relative frequency when averaged over ten days. From the integral of equation (27) this implies that the tangential component of the position error ($\overrightarrow{X_c X_c'}$ in (27)) cumulated over ten days needs to remain below one kilometer (including for example the linear term along the tangential axis in (28)). This is unlikely to raise any difficulty, if the much more stringent requirements from periodic or random errors (see above) are met.

We note that the accuracy requirement is related to a requirement on the knowledge and conservation of the total energy of the orbit. An error in the total energy will show up as a velocity bias, and thus as a linear term along the tangential axis. The non-conservation of the total energy (non-gravitational accelerations) was found to be negligible in section 4. Nonetheless possible long-term effects, if they exist, will lead to a slow variation of the tangential error. The constraint on both, the error in the total energy and the effects due to energy non-conservation is provided by the accuracy requirement, i.e. that the tangential error cumulated over ten days needs to remain below one kilometer.

7. Conclusion

We have derived detailed and general (within the specified assumptions) expressions for the calculation of the effect of orbit determination and instrumental calibration errors on the stability and accuracy of ground to space clock comparisons. These expressions were then used on the specific example of the ACES mission to derive maximum allowed errors given the stability requirements of that mission. For that purpose we have used two simplified orbit error models (Hill model, and random noise), setting limits on the appropriate parameters of those models. Although neither of those models is likely to correctly reflect all of the ISS orbit errors, they are nonetheless expected to provide correct orders of magnitude for the maximum allowed orbit determination uncertainties. They are summarized in table 1, where in each column we have provided the more stringent result from the two models.

Furthermore, we have identified an optimal way to combine upwards and downwards signals (the Λ configuration), which allows for the maximum orbit determination errors. This then provides a constraint on the maximum allowed value of $T_{23} \leq 10^{-6}$ s and its maximum allowed uncertainty of $\delta T_{23} \leq 10^{-7}$ s, which constrains the required knowledge of the sum (transmission + reception) of instrumental delays between the antenna phase centre and the onboard clock (also provided in table 1).

Table 1. Requirements on orbit determination and internal delay calibration

δR /m	δT /m	δN /m	δT_{23} /s
8	16	1400	10^{-7}

Finally, the accuracy requirement of ACES was used to constrain long term ($\approx$ 10 days) linear drifts and other slow variations of the orbit determination errors. We find that the total tangential error cumulated over 10 days needs to stay below 1 km to comply with the accuracy specification (10^{-16} in relative frequency after ten days averaging), which should pose no particular problems given the more stringent short term requirements (see table 1).

In conclusion the requirements on orbit determination are significantly less stringent than the initial 'naive' estimate (one meter error for 10^{-16} in relative frequency), which is mainly due to partial cancelation between the gravitational redshift and the second order Doppler effect in the relativistic frequency correction of the onboard clock.

Acknowledgements. The research project is supported by the French space agency CNES and ESA through Loïc Duchayne's research scholarship *N^o* 05/0812.

References

[Allan D.W. and Ashby N. 1986] Allan D.W. and Ashby N., in: Kovalevsky J., Brumberg V.A. (eds.), Relativity in Celestial Mechanics and Astronomy. Proceedings of the IAU Symposium No. 114 Leningrad 1985, Reidel Publ., Dordrecht (1986).

[Bahder T. B. 2003] Bahder T. B., Phys. Rev. D, **68**, 063005 (2003).

[Bassiri S. and Hajj G. A. 1993] Bassiri S. and Hajj G. A., ISSN 0065-3438, p. 1071-1086 (1993).

[Bize S. et al. 2005] Bize S. et al., J. Phys. B: At. Mol. Opt. Phys., **38**, S449 (2005).

[Bjerhammar A. 1985] Bjerhammar A., Bull. Geod., **59**, 207 (1985).

[Blanchet L. et al. 2001] Blanchet L. et al., Astronomy and Astrophysics, **370**, 320 (2001).

[Colombo O. L. 1986] Colombo O. L., Bulletin géodésique,**60**, 64 (1986).

[Colombo O. L. et al. 2004] Colombo O. L. et al., Proceedings of the Institute Of Navigation GNSS Meeting (2004).

[Duchayne L. 2008] Duchayne L., Ph.D. dissertation (in French), available on http://tel.archives-ouvertes.fr/index.php (2008).

[Heavner T.P. et al. 2005] Heavner T.P. et al., Metrologia, **42**, 411 (2005).

[Klioner S.A. 1992] Klioner S.A., Celestial Mechanics and Dynamical Astronomy, **53**, 81 (1992).

[Linet B. and Teyssandier P. 2002] Linet B. and Teyssandier P., Phys. Rev. D, **66**, 024045 (2002).

[Oskay W.H. et al. 2006] Oskay W.H. et al., Phys. Rev. Lett., **97**, 020845 (2006).

[Petit G. and Wolf P. 1994] Petit G. and Wolf P., Astronomy and Astrophysics, **286**, 971 (1994).

[Rosenband T. et al. 2008] Rosenband T. et al., Science, **319**, 1808, (2008).

[Shapiro I. I. 1964] Shapiro I. I., Phys. Rev. Lett., **13**, 789-791 (1964).

[Soffel M. et al. 1998] Soffel M. et al., Manuscripta Geodetica, **13** 143 (1988).

[Soffel M. et al. 2003] Soffel M. et al., Astronomical Journal, **126**, 2687 (2003).

[Wolf P. and Petit G. 1995] Wolf P. and Petit G., Astronomy and Astrophysics, **304**, 653 (1995).